Nucleic Acids Research, 2017 **1**
doi: 10.1093/nar/gkx655

The abundance of Fob1 modulates the efficiency of rRFBs to stall replication forks

Alicia Castán, Pablo Hernández, Dora B. Krimer and Jorge B. Schvartzman*

Department of Cellular and Molecular Biology, Centro de Investigaciones Biológicas (CSIC), Ramiro de Maeztu 9, 28040 Madrid, Spain

Received January 12, 2017; Revised July 13, 2017; Editorial Decision July 15, 2017; Accepted July 17, 2017

ABSTRACT

In eukaryotes, ribosomal genes (rDNA) are organized in tandem repeats localized in one or a few clusters. Each repeat encompasses a transcription unit and a non-transcribed spacer. Replication forks moving in the direction opposite to transcription are blocked at specific sites called replication fork barriers (rRFBs) in the non-transcribed spacer close to the 3′ end of the transcription unit. Here, we investigated and quantified the efficiency of rRFBs in *Saccharomyces cerevisiae* and to this end transfected budding yeast cells that express dissimilar quantities of Fob1 with circular minichromosomes containing different copies of the minimal 20-bp DNA segment that bind Fob1. To identify fork stalling we used high-resolution 2D agarose gel electrophoresis. The results obtained indicated that neighbor DNA sequences and the relative abundance of Fob1 modulate the efficiency of rRFBs to stall replication forks.

INTRODUCTION

The replication and dynamics of the tandem repeats of ribosomal genes (rDNA) have attracted the attention of biologists for decades. Their study experimented an unexpected twist in 1988 with the discovery of polar ribosomal replication fork barriers (rRFBs). In *Saccharomyces cerevisiae* these rRFBs block only those replication forks moving in the direction opposite to transcription at the non-transcribed spacer close to the 3′ end of the transcription unit (1,2). This discovery was rapidly confirmed in almost all plants and animals studied so far (3). The polar blockage of replication forks depends upon binding of a specific protein: Fob1 in the budding yeast (4). Curiously, this polar blocking depends upon binding of different proteins in *Schizosaccharomyces pombe* (5–8) and mammalian cells (9–13). In summary, the polar blockage of replication forks at rDNA genes is a conserved feature although the proteins responsible are not. Blockage of replication forks prompts genetic recombination (14) and is responsible for the expansion and contraction of rDNA repeats (15). This phenomenon is known as a general feature for ribosomal genes since 1986 (16). The direct correspondence of rRFBs and genetic recombination, though, is not yet fully understood (17) and is known to be tightly regulated (18). On the other hand, replication fork stalling upon collision of transcription and replication was reported earlier for tRNA genes in the budding yeast (19). In *S. pombe* rDNA, though, three closely spaced rRFBs were precisely mapped (6–8) and a fourth replication fork pausing signal due to the collision of transcription and replication was observed as well (5). This observation indicates that in *S. pombe* chromosomes *in vivo* some replication forks are able to go beyond three consecutive programmed barriers before reaching the 3′ end of the transcription unit, suggesting that at least in *S. pombe*, rRFBs are rather inefficient to stall replication forks. The rDNA of *S. cerevisiae* is probably the best characterized so far (20). In this species ∼150 tandem repeats of ∼9.1 kb rDNA units form a single cluster on chromosome XII (21). An autonomous replication sequence (ARS) occurs in the non-transcribed unit of every repeat (Figure 1). All ARSs are potential replication origins but in the chromosomal *locus in vivo* initiation of replication occurs in only ∼20% of the repeats (22) at those ARSs located immediately downstream transcribed genes (23). It is generally accepted that collision of transcription and replication is detrimental (24–26) and the presence of polar rRFBs near the 3′ end of the transcription unit (see Figure 1B) is thought to have developed to prevent such collisions (13,14). For this reason, replication of rDNA is assumed to proceed in a predominantly unidirectional manner (Figure 1A). Three consecutive 20-bp sequences that putatively bind Fob1 (RFB1, RFB2 and RFB3) were precisely mapped (27) in the region comprising the yeast rRFBs (Figure 1C). RFB2 and RFB3 are located 17 bp apart while 40 bp distances RFB1 and RFB2. Brewer *et al.* (28) were the first to identify two pausing sites at the rRFB region of *S. cerevisiae*. They specifically wrote: 'If the rDNA RFB is the consequence of bound protein, it seems likely that there are at least two binding sites in the 129-bp HindIII-HpaI fragment, since forks arrest at two closely spaced sites'. In 1996, Kobayashi and Horiuchi (4) identified a yeast gene product, Fob1 protein, re-

*To whom correspondence should be addressed. Tel: +34 91 837 3112 (Ext 4232); Fax: +34 91 536 0432; Email: schvartzman@cib.csic.es

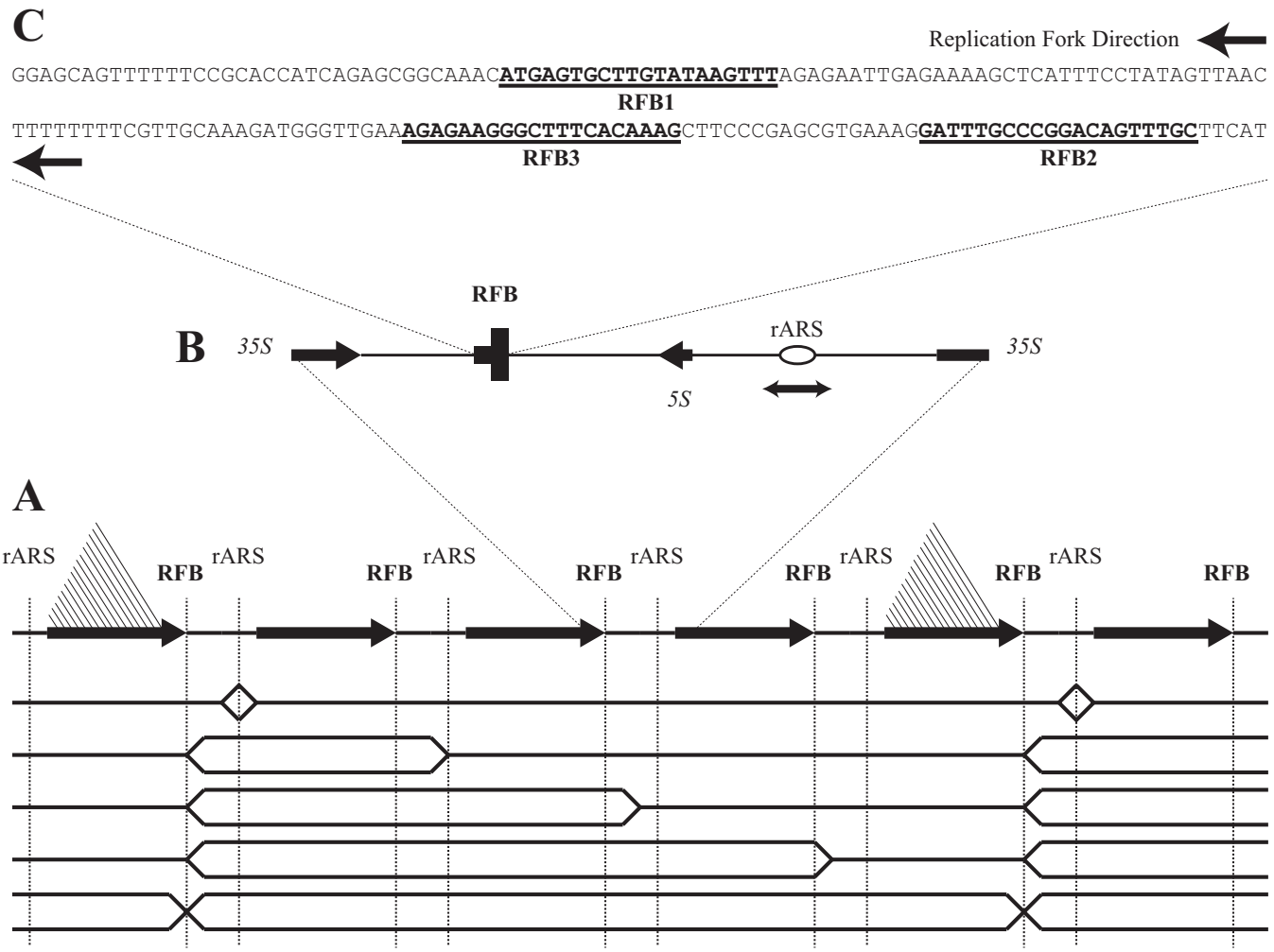

Figure 1. Cartoons illustrating the organization and functioning of rDNA tandem repeats in the budding yeast. (**A**) On top, thick arrows represent the 35S transcriptional units separated by thinner lines representing the non-transcribed spacers. Broken vertical lines indicate the location of replication origins and polar replication fork barriers (RFBs). Half Christmas trees indicate two transcriptionally active 35S units. Replication of the locus is illustrated below. Initiation only occurs immediately downstream transcriptionally active units. Replication proceeds bi-directionally but the fork moving leftward stalls at the first RFB encountered. The fork moving rightward progresses unconstrained until it meets another fork stalled at an RFB. (**B**) Higher resolution of a non-transcribed spacer showing its most relevant components: the 3′ end of the left 35S neighbor unit, the polar RFB, location and transcription orientation of the 5S gene, the bi-directional replication origin and the 5′ end of the right 35S neighbor unit. (**C**) DNA sequence of the 186-bp subfragment 7 described by Kobayashi (20) with the three putative Fob1 binding sites (RFB1, RFB2 and RFB3) highlighted. Arrows indicate the direction of replication forks that would be stalled.

quired for both replication fork blocking and recombinational hotspot activities in the rDNA of *S. cerevisiae*. Ward *et al*. (17) re-examined the fork stalling capacity within this 129-bp HindIII-HpaI fragment. They performed systematic mutagenesis of 10-bp consecutive segments and two-dimensional (2D) agarose gel electrophoresis to reveal only two pausing sites within this region. However, they specifically emphasized that 'sequences that lie *35S* gene-proximal to the HindIII site contributed to RFB activity. In addition to the HindIII-HpaI fragment, sequences within the 188-bp EcoRI-HindIII fragment most likely comprise the region sufficient for full RFB2 activity'. A couple of years later, Kobayashi (27) identified three potential Fob1 binding sites in the rRFB Fob1 associating region of *S. cerevisiae*, named RFB1, RFB2 and RFB3. He consciously extended his study to sequences lying *35S* gene-proximal to the HindIII site. He concluded: 'I detected neither RFB activity nor Fob1 association of the RFB2 fragment, although RFB2 did interact with Fob1 in the footprinting assay (Figure 5A). From these data, I speculate that the second spot observed in the 2D analysis is the sum of RFB2 and RFB3 activities and that for the activity of RFB2, Fob1 association with RFB3 is necessary. This association makes it possible that RFB2 interacts with Fob1 to inhibit replication'. Altogether, these observations imply that the precise nature and number of barriers at the budding yeast rDNA remain confuse and should be solved.

We wanted to confirm the number of barriers at the budding yeast rRFBs and know more about their efficiency to stall replication forks not in their natural chromosomal context but in extra-chromosomal elements. To this end we transfected *S. cerevisiae* cells with circular

minichromosomes containing different copies of the minimal DNA segment that is known to bind Fob1 (27). To identify fork stalling we used high-resolution 2D agarose gel electrophoresis (2D gels) to analyze the replication intermediates (RIs) of two different restriction fragments where stalling occurs at different relative sites. Several features of the immunograms are important to notice. First, this technique allows detection of different patterns of RIs (29,30): containing an internal bubble (drawn in red in Figure 2), simple-Ys (drawn in green) and double-Ys (drawn in magenta). Two different patterns denote unreplicated molecules. They correspond to linear fragments generated by non-specific hybridization and DNA breakage during isolation (drawn as an unbroken black baseline) and the so-called X-shaped recombinant arc (drawn in light blue). Replication fork stalling generates a prominent spot on the simple-Y arc. This prominent spot may be located before or after half of the molecule completed its replication (indicated by a green arrow in Figure 2). If fork stalling were transitory, the simple-Y signal continues beyond the prominent spot indicating a pause. On the other hand, if fork stalling were permanent, a transition from simple-Ys to double-Ys takes place, as once progression of the first fork is blocked, the only way to complete replication of the fragment is by means of another (second) fork traveling in the opposite direction (indicated by broken thick magenta lines in Figure 2). Appearance of this second fork generates a double-Y signal that extends between a position on the simple-Y arc (green filled black circles) and a position on the arc of X-shaped recombinants (magenta filled black circles). If the transition from single- to double-Ys occurs after half of the molecule was replicated, the double-Y signal extends as a straight line. On the other hand, if the transition occurs before half of the molecule completed its replication, the double-Y signal shows an inflection (30–32). Termination occurs when the second fork meets the first blocked one. At this time, the shape of the last RI resembles an X-shaped recombinant in regard to electrophoretic mobility. The meeting of both forks moving in opposite directions on the arc of X-shaped recombinants maps the termination site between the middle of the fragment (0.50) and either one of the ends (0.00).

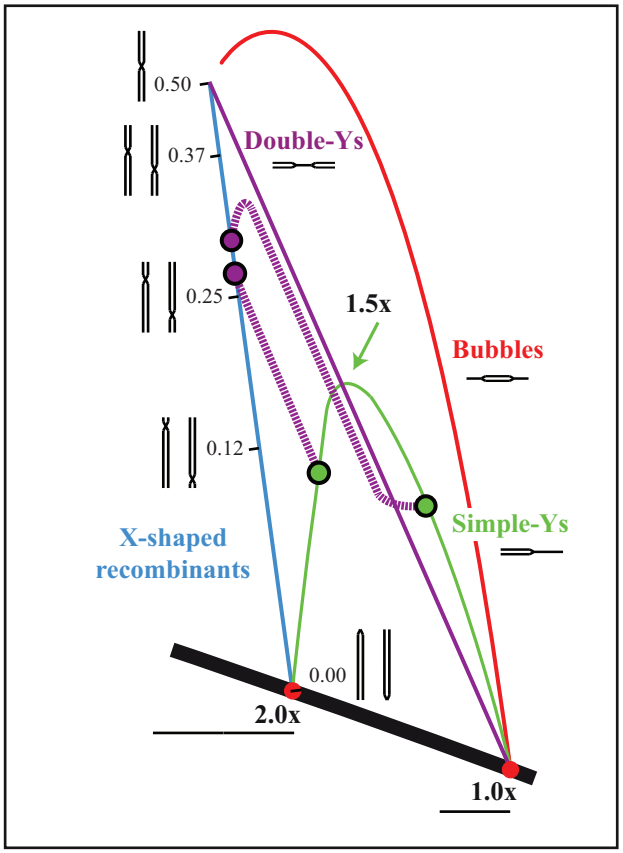

Figure 2. Cartoon illustrating the different patterns of RIs corresponding to a linear DNA fragment identified in 2D gels. Two of the signals observed are generated by non-replicating molecules. They are linear fragments of different sizes with high electrophoretic mobility that move to the bottom (indicated by a thick black line). On top of this signal red dots indicate unreplicated (1.0×) and almost fully replicated (2.0×) forms of the fragment under study. X-shaped recombinants (indicated by a thin light blue line) corresponds to two identical fragments linked by a Holliday-like junction located somewhere along them. If the Holliday junction is located precisely in the middle, the molecule has four identical arms (indicated as 0.50). If it is located almost at the end, the molecule resembles a linear 2.0× fragment (indicated as 0.00). Intermediate positions are indicated as 0.12, 0.25 and 0.37. Bi-directional initiation from an origin located in the middle of the fragment generates a series of RIs named 'bubbles' (indicated in red). The pattern generated by a single fork initiated outside the fragment that progresses from one end to the other is called 'simple-Ys' (indicated in green). The pattern generated by two forks initiated outside the fragment that progress against each other is called 'double-Ys' (indicated in magenta). If one of the forks gets to the fragment ahead of the other a transition from simple-Y to double-Y takes place. Transitions occur when the RIs achieve a specific mass. When the fork then enters the fragment first stalls, if the mass of the RI with the stalled fork is bigger than 1.5× the double-Y pattern extends as a straight line connecting a point on the descending portion of the simple-Ys (indicated by a green-filled black circle) to another point on the X-shaped recombinant arc (indicated by a magenta-filled black circle). On the contrary, if the mass of the RI with the stalled fork is smaller than 1.5× the double-Y pattern extends from a point on the ascending portion of the simple-Y arc to another point on the X-shaped recombinant arc. In this case, the double-Y pattern shows an inflection that marks the middle of the segment replicated as a double-Y (indicated with a light blue arrow and vertical broken line in Supplementary Figures S2–4).

MATERIALS AND METHODS

Construction of minichromosomes

- pYAC_MEM (7966 bp): described in (33).
- pYAC_MEM_3rRFBs+ (8908 bp): described in (33).
- pYAC_AC_3′rRFBs+ (8175 bp): We synthesized a 209-bp DNA fragment (GeneWiz Service, Sigma) containing the 186-bp subfragment 7 (see Figure 1C) described by Kobayashi (27) where 23 bp were added between RFB2 and RFB3 (underlined in the following DNA sequence): GTTAACTATAGGAAATGAGCTTTT CTCAATTCTCTAAACTTATACAAGCACTCA TGTTTGCCGCTCTGATGGTGCGGAAAAAAC TGCTCCATGAAGCAAACTGTCCGGGCAAAT CCAAGTGGTATTCCGTAAGAACAACTTTCACG CTCGGGAAGCTTTGTGAAAGCCCTTCTCTTTC AACCCATCTTTGCAACGAAAAAAAA. This DNA

fragment was inserted into the unique SalI site of the pYAC_MEM.
- pYAC_AC_10rRFBs+ (8914 bp): first, we synthesized a 948-bp DNA fragment (GeneWiz Service, Sigma) containing five tandem repeats of the 186-bp subfragment 7 (see Figure 1C) described by Kobayashi (27). This fragment was inserted into the unique SalI site of pYAC_MEM.

DNA transfection

DNA isolated from *Escherichia coli* cells was introduced into budding yeast cells by the lithium acetate method (34).

Yeast strains

Three different strains of *S. cerevisiae* were used: (i) top2-td (supplied by Jonathan Baxter) was based on W303-1A (*MATa leu*2-3/112 *ura*3-1 *trp*1-1 *his*3-11/15 *ade*2-1 *can*1-100) modified as described in (35); (ii) GAL-3HA-FOB1 (*MATa his3Δ1 leu2Δ met15Δ ura3Δ Gal-Fob1-3HA*) containing an inducible galactose promoter upstream the native *FOB1* promoter and three hemagglutinin (HA) epitope tags downstream and (iii) BY4741 (the GAL-3HA-FOB1 wild-type isogenic strain). The last two strains were supplied by Luis Aragón.

Culture media and cell synchronization

Cells were grown at the appropriate temperature in synthetic medium without uracil containing 2% raffinose. Cultures were transferred to complete YEP medium with raffinose until midlog and cells were arrested in G1 with 5 μg/ml α-factor. Induction of the galactose promoter was achieved by addition of 2% galactose. When 90% of cells were in G1 (120–150 min) cells were washed four times and incubated in YEP medium with 2% raffinose (plus 2% galactose in the induction case). Cells were harvested at the indicated times. Time 0 was defined as the time of the first wash. Cells synchronization was performed as described in (36).

DNA isolation

To isolate DNA enriched for RIs, samples were prepared according to Huberman's procedure (37) with some modifications (38,39).

DNA treatments

DNA was digested with the restriction endonucleases BamHI, EcoRV, SwaI, FspI and MluI (New England Biolabs) for at least 2 h at 37°C except for SwaI that was digested at 25°C.

2D agarose gel electrophoresis and southern transfer

The first dimension was in a 0.4% agarose gel (Seakem® LE; Lonza) in TBE buffer (89 mM Tris-borate, 2 mM ethylenediaminetetraacetic acid) at 0.9 V/cm at room temperature for 24–27 h. The second dimension was in a 1–1.2% agarose gel in TBE buffer and was run perpendicular to the first dimension. The dissolved agarose was poured around the excised agarose lane from the first dimension and electrophoresis was at 4.5 V/cm in a 4°C cold chamber for 10–12 h. in the presence of 0.3 μg/ml ethidium bromide. Southern transfer was performed as described before (38,39).

Non-radioactive hybridization

DNA probes were labeled with digoxigenin using the DIG-High Prime kit (Roche). Membranes (Zeta-Probe GT membranes, Bio-Rad) were pre-hybridized in a 20 ml pre-hybridization solution (2× SSPE, 0.5% Blotto, 1% sodium dodecyl sulphate (SDS), 10% dextran sulphate and 0.5 mg/ml^{-1} sonicated and denatured salmon sperm DNA) at 65°C for 4–6 h. Labeled DNA was added and hybridization lasted for 12–16 h. Hybridized membranes were sequentially washed with 2× Saline sodium citrate (SSC) and 0.1% SDS at room temperature for 5 min twice and with 0.1× SSC and 0.1% SDS at 68°C for 15 min twice as well. Detection was performed with an antidigoxigenin-AP conjugate antibody (Roche) and CDP-Star (Perkin Elmer) according to the instructions provided by the manufacturer.

Immunoblot analysis

GAL-3HA-FOB1 cells were lysed with 20% trichloroacetic acid. Proteins were separated by 12% SDS-polyacrylamide gel electrophoresis and transferred to a poly-1,1-difluoroethene (PVDF) membrane (BioRad). The membranes were incubated with mouse monoclonal anti-HA antibody (Roche) and mouse monoclonal anti-PSTAIR (Sigma), followed by Horseradish peroxidase (HRP)-conjugated anti-mouse (Santa Cruz).

RESULTS

To check the number of barriers and their efficiency to stall replication forks in *S. cerevisiae* we used as a control the circular minichromosome named pYAC_MEM that carries no rRFB (33). The genetic map of this minichromosome is shown in Figure 3A. Its most relevant features described clockwise starting with the bidirectional replication origin ARS4 were: the *S. cerevisiae* gene *URA3*, the lambda DNA fragment L1 (used for selective hybridization), the *S. cerevisiae* gene *HIS3*, another lambda DNA fragment named L2, the ColE1 replication origin, the *E. coli* gene for ampicillin resistance and the *S. cerevisiae* centromeric sequences CEN6. The position of specific endonuclease restriction sites is indicated outside the map. This minichromosome was employed to transfect top2-td yeast cells (see 'Materials and Methods' section).

We used high-resolution 2D gels to analyze the RIs of two different linear fragments of this minichromosome. Digestion with the restriction enzymes SwaI and BamHI revealed a 2764-bp DNA linear fragment containing the replication origin and CEN6 (Figure 3A and B) whereas digestion with EcoRV and MluI revealed a 4245-bp linear fragment that contains neither a replication origin nor a centromere (Figure 3A and C). The immunograms of the corresponding 2D gels hybridized with the L1 probe are shown in Figure 3D and F with their corresponding diagrammatic interpretations to their right (Figure 3E and G). Computer simulations using a 2D gel application (40) showed that *in vivo*

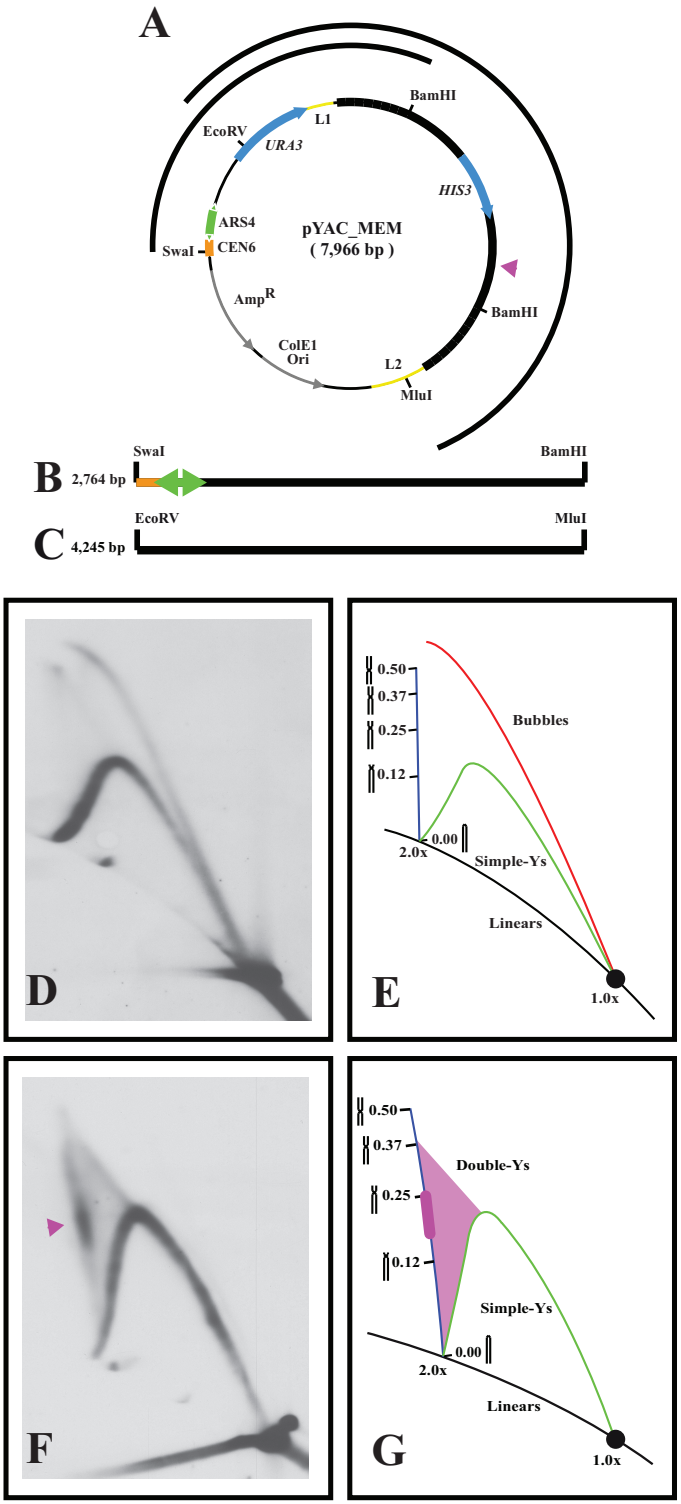

Figure 3. Genetic map and 2D gel analysis of linear fragments corresponding to pYAC_MEM. (**A**) Genetic map of pYAC_MEM (7966 bp) showing its most relevant features: clockwise starting with the replication origin ARS4 (indicated in green), URA3 gene active in *Saccharomyces cerevisiae* (indicated in light blue), L1 lambda DNA used for hybridization (indicated in yellow), HIS3 gene active in *S. cerevisiae* (indicated in light blue), L2 lambda DNA used for hybridization (indicated in yellow), the ColE1 replication origin active only in *Escherichia coli* (indicated in gray), the ampicillin resistance gene active only in *E. coli* (indicated in gray) and the budding yeast centromeric sequence CEN6 (indicated in orange). The sites for specific restriction endonucleases are indicated outside the map. In addition, a magenta triangle points the position located 180° apart from the replication origin ARS4. (**B**) Map of the 2764-bp linear fragment generated by digestion of pYAC_MEM with SwaI and BamHI. (**C**) Map of the 4245-bp linear fragment generated by digestion of pYAC_MEM with EcoRV and MluI. (**D**) 2D gel immunogram of the RIs corresponding to the SwaI-BamHI 2764 bp linear fragment with its diagrammatic interpretation in (**E**). The 2D gel immunogram of the RIs corresponding to the EcoRV-MluI 4245-bp linear fragment is shown in (**F**) with its diagrammatic interpretation in (**G**). De-localized termination signals are indicated in magenta.

replication forks behave in three different ways as they go thru CEN6 (33). In some minichromosomes, the counterclockwise moving fork stalls permanently at CEN6. In others, this fork pauses at CEN6 just briefly although for different periods of time and in some other cases, CEN6 represents no obstacle for replication forks to go by. The results we obtained confirmed all these predictions (Supplementary Figure S1A). A complete simple-Y arc was prominent in the immunogram corresponding to the SwaI-BamHI 2764-bp DNA fragment (Figure 3D and E). This was the expected pattern for unconstrained replication (left series of RIs in Supplementary Figure S1A). An almost complete bubble arc was clearly identified as well (Figure 3D and E). This was the expected pattern when CEN6 act as a permanent barrier (mid series of RIs in Supplementary Figure S1A). In this case transition from bubbles to simple-Ys was expected to occur when the mass of RIs achieved 1.97× to 1.98× (pointed with a red arrow in the mid panel of Supplementary Figure S1A). Termination on the X-shaped recombinant arc would occur close to one end (0.02 in a scale from 0.00 to 0.50). Finally, the extension of the bubble arc and the transition from bubbles to simple-Ys would occur at different positions in different cases depending on how long pausing of the counterclockwise moving fork was at CEN6 (right series of RIs in Supplementary Figure S1A). The 2D gel patterns corresponding to the EcoRV-MluI 4245-bp DNA fragment were clearly different (Figure 3F and G). No bubble arc was visible in this immunogram as the fragment contained no ARS. A complete simple-Y arc was also prominent. This was the expected pattern when CEN6 act as a permanent barrier (mid series of RIs in Supplementary Figure S1B). The termination signal (double-Ys) was noticeably diffuse (Figure 3F and G). A significantly intense section of the X-shaped recombinant arc (pointed with a magenta arrow in Figure 3F) was observed between positions 0.12 and 0.25 as indicated in Figure 3G. This was expected if the replication fork moving counterclockwise proceeded almost unconstrained thru CEN6 and both forks initiated at ARS4 met ∼180° apart between the *HIS3* gene and the bottom BamHI restriction site (pointed with a magenta arrowhead in the complete map of Figure 3A). In addition, a triangular diffuse smear was also observed in the immunogram (Figure 3F and G). This was expected if the transition from single- to double-Ys occurred at different positions in different cases depending on how long pausing of the counterclockwise moving fork was at CEN6 (33,41). Altogether these observations indicated that no molecules replicated uni-directionally from ARS4 in a counterclockwise manner.

Next, we studied a derivative of pYAC_MEM named pYAC_MEM_3rRFBs+. This minichromosome was constructed by inserting the 942 bp EcoRI fragment of pBB6-RFB+ (18,28) containing the *S. cerevisiae* rRFB and flanking sequences into the SalI site of pYAC_MEM in the orientation known to stall replication forks. The inserted fragment encloses the 186-bp subfragment 7 containing the three putative Fob1 binding sites described by Kobayashi (27). The new minichromosome was 8908 bp (Figure 4A). We used this new minichromosome to transfect top2-td yeast cells as well. Digestion with the restriction enzymes SwaI and BamHI and hybridization with the L1 probe revealed a 3708-bp linear DNA fragment containing ARS4 and CEN6 (Figure 4A and B) whereas digestion with EcoRV and MluI revealed a 5186-bp linear fragment devoid of origins and centromeres (Figure 4A and C). The immunograms of the corresponding 2D gels are shown in Figure 4D and F with their corresponding diagrammatic interpretations to their right (Figure 4E and G). Computer simulations using the 2D gel application (40) showed the shape and mass of the different RIs expected (Supplementary Figure S2). In addition to the patterns already identified for the SwaI-BamHI linear fragment corresponding to pYAC_MEM shown in the immunogram of Figure 3D, here two prominent spots were detected on top of the descending portion of the simple-Y arc (green filled black circles pointed with small arrows numbered 1 and 2 in the diagrammatic interpretation of Figure 4E). Two prominent spots were detected also on top of the X-shaped recombinant arc (blue filled black circles in the diagrammatic interpretation of Figure 4E). Two thin straight signals connected the green-filled black spots on the simple-Y arc with the blue-filled black spots on the X-shaped recombinant arc. Note that only two, not three spots were detected in the immunograms (see the densitometric profile in Figure 4H). Note that the first spot generated by the advancing fork was slightly more intense than the second. In this case, computer simulations using the 2D gel application (40) predicted three accumulation spots (RFB1, RFB2 and RFB3) provided the three putative Fob1p binding sites were able to block fork progression (see the three right panels in Supplementary Figure S2A).

The 2D gel patterns corresponding to the EcoRV-MluI 5186-bp DNA fragment were clearly different (Figure 4F and G). Once again, in addition to the patterns already identified for the EcoRV-MluI fragment corresponding to pYAC_MEM shown in the immunogram of Figure 3F, here two prominent spots were detected also on top of the simple-Y arc but in this case on its ascending portion (green filled black circles pointed with small arrows numbered 1 and 2 in the diagrammatic interpretation of Figure 4G). Two prominent spots were detected on top of the X-shaped recombinant arc, too (blue filled black circles in the diagrammatic interpretation of Figure 4G). Here, though, the signals connecting the green-filled black spots on the simple-Y arc with the blue-filled black spots on the X-shaped recombinant arc showed an inflection close to the arc of X-shaped recombinants. It should be noticed that the computer simulation of the shape and mass of the RIs expected (Supplementary Figure S2B) predicted that for this fragment, unconstrained replication would allow both forks to meet around position 0.30 on the X-shaped recombinant arc. Permanent blockage of the counterclockwise moving fork at CEN6 would lead to a complete simple-Y arc. Finally, stalling of the clockwise moving fork at the RFBs would take place before the mass of the RIs achieved 1.5×. Therefore, if fork stalling were permanent, termination would occur when another fork moving in the opposite direction meets the blocked one precisely at the rRFBs. In this case, termination would occur around positions 0.29, 0.30 and 0.32, respectively, on the arc of X-shaped recombinants (see the three right panels in Supplementary Figure S2B). The significantly intense section on the X-shaped recombinant arc (pointed with a magenta arrow in Fig-

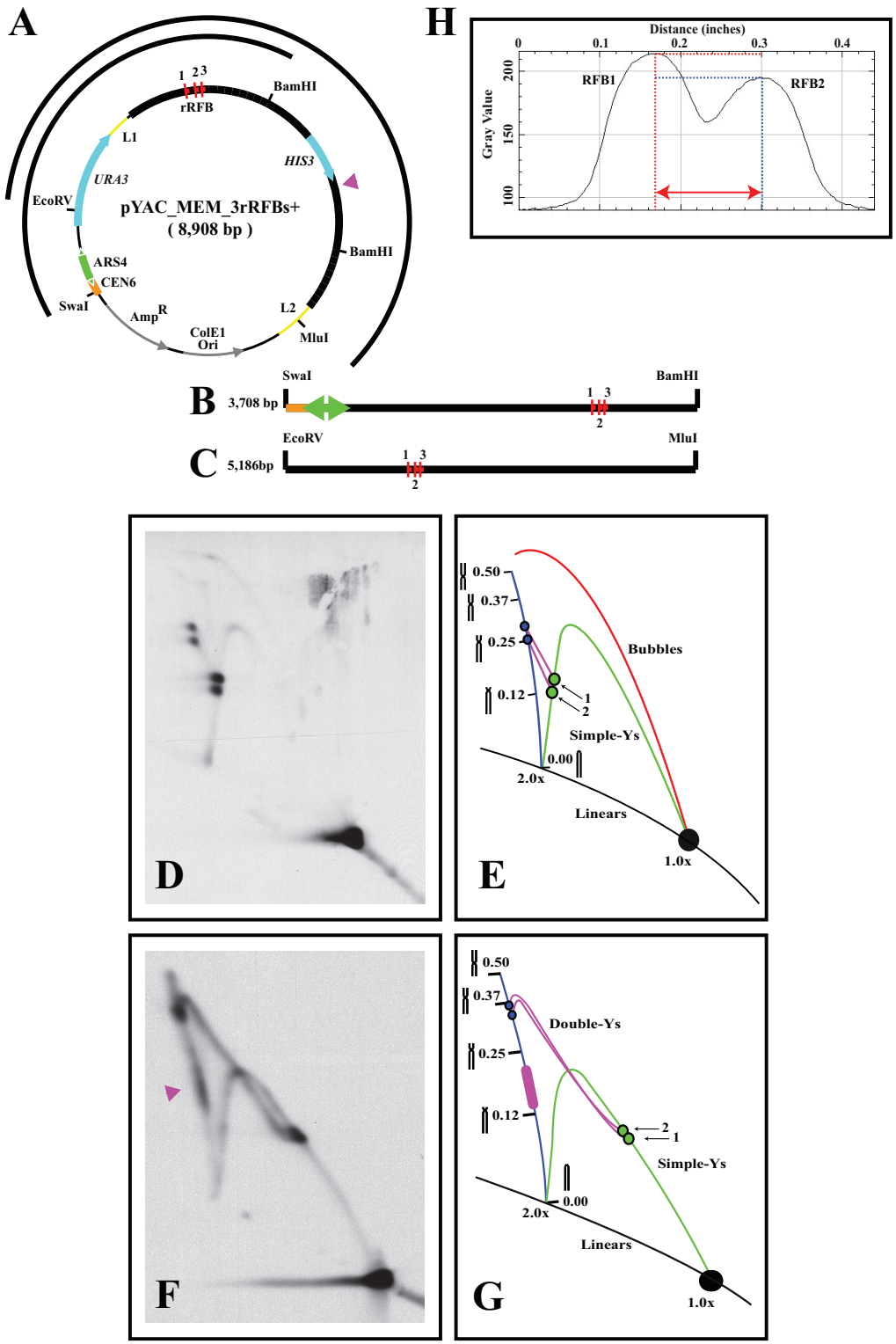

Figure 4. Genetic map, 2D gel analysis of linear fragments corresponding to pYAC_MEM_3rRFBs+ and densitometry of the spots accumulated on the simple-Y arc. (**A**) Genetic map of pYAC_MEM_3rRFBs+ (8908 bp) showing its most relevant features (for further details see the legend of Figure 3). Note the insertion of an EcoRI fragment containing the three putative Fob1 binding sites expected to act as RFBs (indicated in red), described by Kobayashi (20). (**B**) Map of the 3708 bp linear fragment generated by digestion of pYAC_MEM_3rRFBs+ with SwaI and BamHI showing the relative position of the three putative RFBs. (**C**) Map of the 5186 bp linear fragment generated by digestion of pYAC_MEM_3rRFBs+ with EcoRV and MluI showing the relative position of the three putative RFBs. (**D**) 2D gel immunogram of the RIs corresponding to the SwaI-BamHI 3708 bp linear fragment with its diagrammatic interpretation in (**E**). The 2D gel immunogram of the RIs corresponding to the EcoRV-MluI 5186-bp linear fragment is shown in (**F**) with its diagrammatic interpretation in (**G**). The densitometric profile corresponding to the spots observed on the simple-Y arc shown in (D) is presented in (**H**) indicating the height of the peaks and the distance separating them.

ure 4F) was also observed in this case but now closer to position 0.12 as indicated in Figure 4G. As in the case of pYAC_MEM, this was expected if the replication fork moving counterclockwise proceeded almost unconstrained thru CEN6 and both forks initiated at ARS4 met approximately 180° apart near the 3′ end of the *HIS3* gene (pointed with a magenta arrowhead in the complete map of Figure 4A). Note that only two, not three spots were detected in this immunogram, too.

We noticed that the number of base pairs separating RFB1 and RFB2 (40 bp) was larger than the 17 bp separating RFB2 and RFB3 (see Figure 1). It could be argued that only two accumulation spots were detected in the immunograms shown in Figure 4 because the 2D gel conditions here used were unable to resolve blockage of the forks at too closely spaced sites. To test this possibility, we constructed a new minichromosome, pYAC_AC_3′rRFBs+, where the distance between RFB2 and RFB3 was increased and made identical to the distance between RFB1 and RFB2, exactly 40 bp. We used this minichromosome to transfect top2-td yeast cells as well. The genetic map and corresponding 2D gel immunograms are shown in Figure 5. In this case, to analyze a fragment containing the replication origin, the centromere and the rRFBs of a size comparable to the 3708-bp SwaI-BamHI fragment analyzed from pYAC_MEM_3rRFBs+, pYAC_AC_3′rRFBs+ was digested with FspI and BamHI. The new linear fragment generated containing the replication origin, the centromere and the rRFBs was 3710 bp. Note that here too, only two accumulation spots were detected in pYAC_AC_3′rRFBs+. Moreover, the densitometric profile of the spots observed on the simple-Y arcs shown in Figure 5H clearly showed that the relative distance between the two spots has increased compared to pYAC_MEM_3rRFBs+ (see the densitometric profiles shown in Figure 5H). This was observed also for the spots on the X-shaped recombinant arcs (densitometric profiles not shown). In addition, we noticed that for both minichromosomes the spot generated by RFB1 (the first one encountered by clockwise moving forks) was undoubtedly more robust that the spot generated by RFB2. The shape and mass of the expected RIs are shown in Supplementary Figure S3. The results obtained clearly indicated that the putative Fob1 binding site formerly named RFB2 did not act as a polar replication fork-blocking site *in vivo*. In consequence, from now on we will refer to the active budding yeast barriers as rRFB1 and rRFB2.

One of the most important observations revealed in the immunograms showed in Figures 4 and 5 was the detection of a complete simple-Y signal regardless of fork blockage. This observation indicated that in the minichromosomes studied, a number of replication forks were able to go beyond the putative RFBs apparently undisturbed. Moreover, the detection of signals corresponding to double-Ys indicated that in those cases where replication forks were blocked at the RFBs, termination of DNA replication took place by means of another fork moving in the opposite direction. In other words, these observations suggested that blockage of replication forks at the budding yeast's rRFBs when occurred were permanent, but this blockage did not occur in all cases.

Would it be possible to improve the efficiency of rRFBs so that all replication forks would be blocked? In a first attempt to answer this question we constructed a new minichromosome named pYAC_AC_10rRFBs+. We synthesized a 948-bp DNA fragment containing five tandem repeats of the 186 bp subfragment 7 (see Figure 1C) described by Kobayashi (27). This fragment was inserted at the unique SalI site of pYAC_MEM in the orientation known to stall replication forks. The inserted fragment contained the 10 Fob1p binding sites described by Kobayashi (27) that here we confirmed act as RFBs *in vivo* (See Figures 4 and 5). The new minichromosome was 8916 bp (Figure 6A). We used this minichromosome to transfect top2-td yeast cells as well. The genetic map and corresponding 2D gel immunograms of the same restriction digests used before are shown in Figure 6. Note that ten accumulation spots were detected in pYAC_AC_10rRFBs+ on the simple-Y arc as well as on the X-shaped recombinant arc in both digests (Figure 6D and F). Moreover, the densitometric profile of the spots detected on the simple-Y arc shown in Figure 6D indicated that here the last spot encountered by the replicating fork (RFB10) appeared slightly stronger than the others. The pattern was similar regardless the fragment analyzed (Figure 6D and F). The shape and mass of the expected RIs are shown in Supplementary Figure S4.

However, a complete simple-Y arc was still detected indicating that some forks moving clockwise were able to go beyond 10 successive Fob1 potential binding sites with no apparent difficulty. In other words, it appears not all the potential Fob1 binding sites actually bound the protein. This could be due to a shortage of Fob1 in the budding yeast strain we used. In an attempt to increase Fob1 availability we used the same 8916-bp minichromosome (pYAC_AC_10rRFBs+) to transfect another yeast strain (GAL-3HA-FOB1) that contained the *GAL* promoter upstream the native *FOB1* promoter and three HA epitope tags downstream. We confirmed Fob1 was indeed overexpressed in these cells in the presence of galactose (data not shown). The 2D gel immunograms of the same restriction digests used so far are shown in Figure 7D and F. To our surprise a complete simple-Y arc was still detected in both cases. In addition, the intensity of the 10 spots changed significantly. A comparison of the densitometric profiles corresponding to the spots on the simple-Y arc obtained for the 3705-bp SwaI-BamHI linear DNA fragment isolated from top2-td and GAL-3HA-FOB1 cells is shown in Figure 7H. Note that the peaks corresponding to RFB 5, 7 and 9 were similar and flat for the DNA isolated from top2-td cells whereas they were distinctly prominent for the DNA isolated from GAL-3HA-FOB1 cells. Note also the inversion of intensities between the peaks corresponding to RFB 9 and 10. To confirm that the differences observed were due to *FOB1* overexpression, the GAL-3HA-FOB1 isogenic strain BY4741 was transformed with pYAC_AC_10rRFBs+ and the SwaI and BamHI fragment was analyzed in 2D gels. The results obtained indicated unambiguously that the pattern obtained for BY4741 cells closely resembled those obtained for the top2-td strain and were clearly different from those obtained for GAL-3HA-FOB1 cells where *FOB1* was overexpressed (data not shown). These results confirmed that

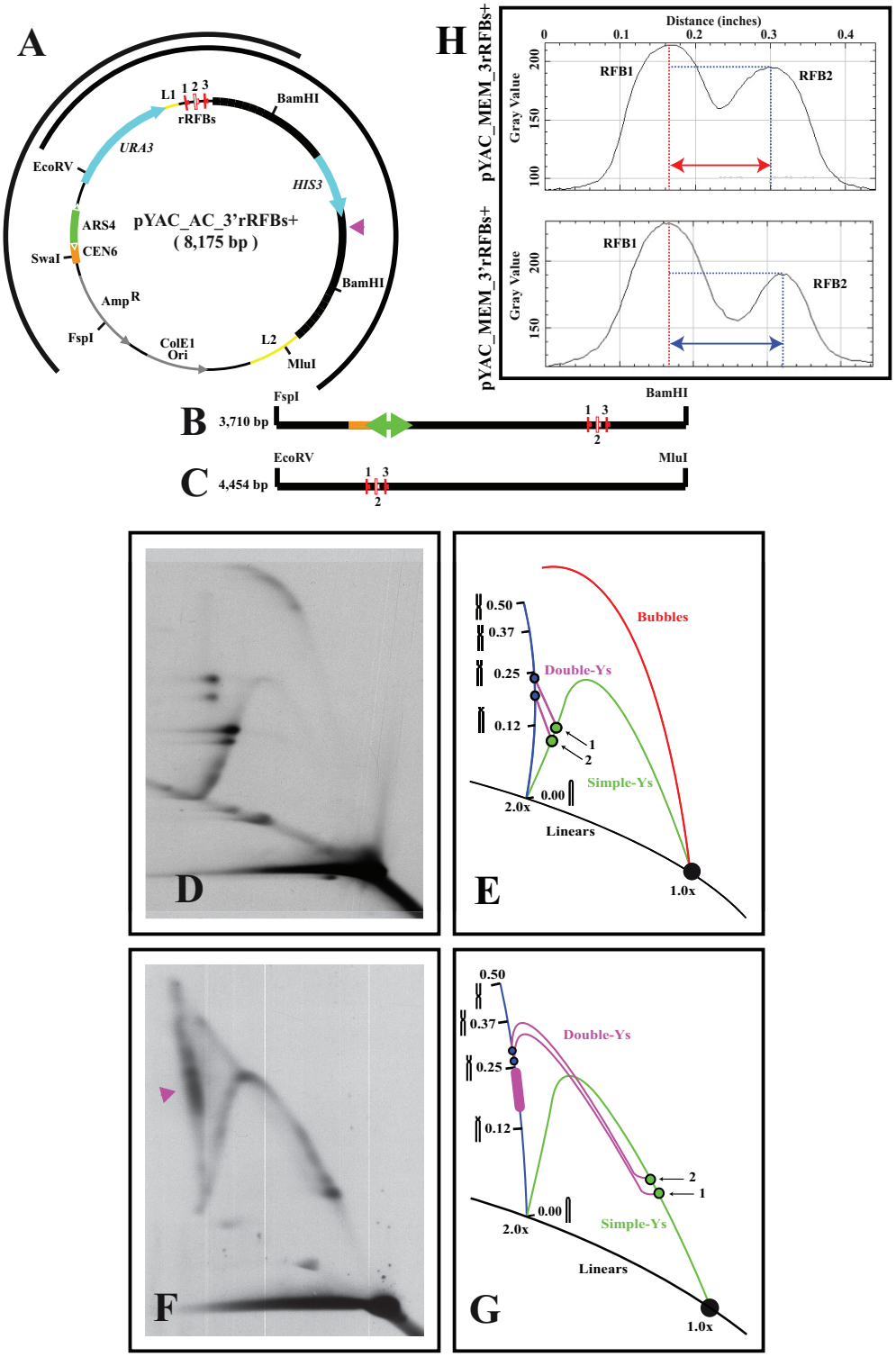

Figure 5. Genetic map, 2D gel analysis of linear fragments corresponding to pYAC_AC_3′rRFBs+ and densitometry of the spots accumulated on the simple-Y arc. (**A**) Genetic map of pYAC_AC_3′rRFBs+ (8175 bp) showing its most relevant features (for further details see the legend of Figure 3). Note that here the three putative Fob1 binding sites expected to act as RFBs (indicated in red and white), described by Kobayashi (20), are equally distanced. (**B**) Map of the 3710-bp linear fragment generated by digestion of pYAC_AC_3′rRFBs+ with FspI and BamHI showing the relative position of the three putative RFBs. (**C**) Map of the 4454-bp linear fragment generated by digestion of pYAC_AC_3′rRFBs+ with EcoRV and MluI showing the relative position of the three putative RFBs. (**D**) 2D gel immunogram of the RIs corresponding to the FspI-BamHI 3710-bp linear fragment with its diagrammatic interpretation in (**E**). The 2D gel immunogram of the RIs corresponding to the EcoRV-MluI 4454-bp linear fragment is shown in (**F**) with its diagrammatic interpretation in (**G**). The densitometric profile corresponding to the spots observed on the simple-Y arc shown in (D) is presented in (**H**) indicating the height of the peaks and the distance separating them. For comparison, the densitometric profile corresponding to pYAC_MEM_3rRFBs shown in Figure 4H is presented on top.

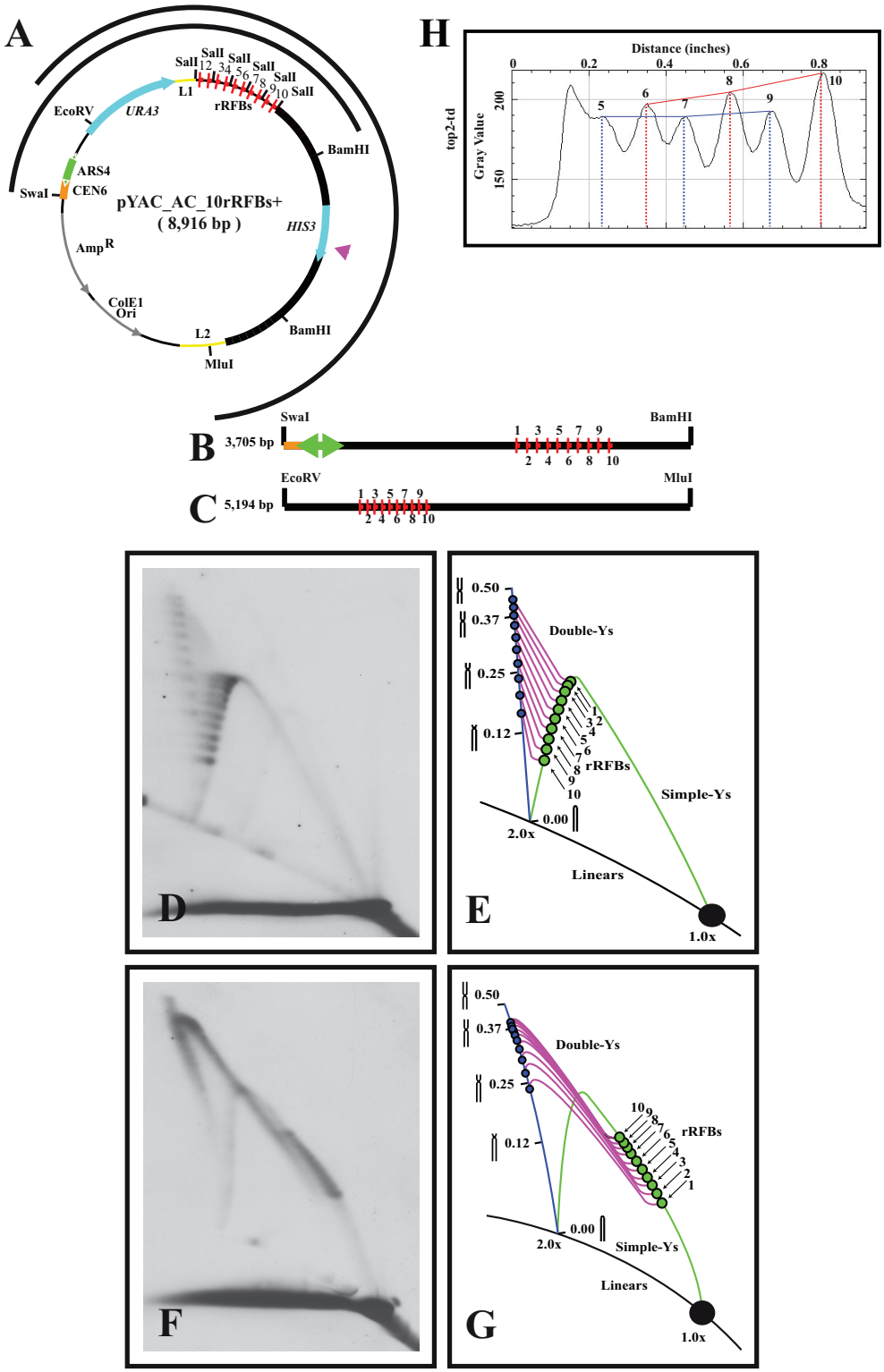

Figure 6. Genetic map, 2D gel analysis of linear fragments corresponding to pYAC_AC_10rRFBs+ and densitometry of the spots accumulated on the simple-Y arc. (**A**) Genetic map of pYAC_AC_10rRFBs+ (8916 bp) showing its most relevant features (for further details see the legend of Figure 3). Note that here the fragment inserted at the unique SalI site of pYAC_MEM contained the 10 Fob1 binding sites described by Kobayashi (20) that were confirmed to act as RFBs *invivo* (See Figures 4 and 5). (**B**) Map of the 3705-bp linear fragment generated by digestion of pYAC_AC_10rRFBs+ with SwaI and BamHI showing the relative position of the 10 putative RFBs. (**C**) Map of the 5194-bp linear fragment generated by digestion of pYAC_AC_10rRFBs+ with EcoRV and MluI showing the relative position of the 10 putative RFBs. (**D**) 2D gel immunogram of the RIs corresponding to the SwaI-BamHI 3705-bp linear fragment with its diagrammatic interpretation in (**E**). The 2D gel immunogram of the RIs corresponding to the EcoRV-MluI 5194-bp linear fragment is shown in (**F**) with its diagrammatic interpretation in (**G**). The densitometric profile corresponding to the six most distal spots observed on the simple-Y arc shown in (D) is presented in (**H**) indicating the height of the peaks.

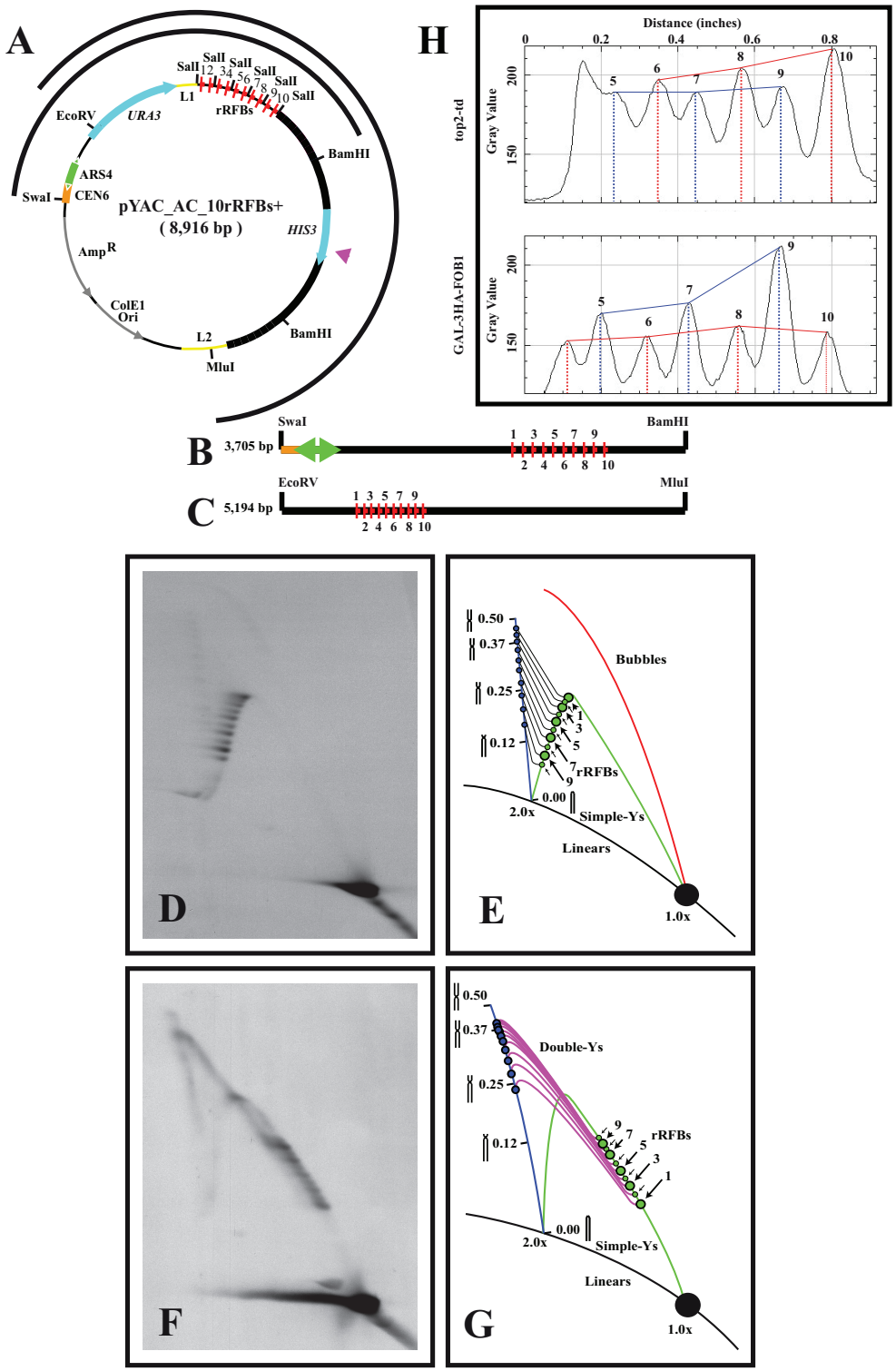

Figure 7. Genetic map, 2D gel analysis of linear fragments corresponding to pYAC_AC_10rRFBs+ isolated from cells that overexpress Fob1 and densitometry of the spots accumulated on the simple-Y arc. (**A**) Genetic map of pYAC_AC_10rRFBs+ (8916 bp) showing its most relevant features (for further details see the legend of Figure 3). Note that here the fragment inserted at the unique SalI site of pYAC_MEM contained the 10 Fob1 binding sites described by Kobayashi (20) that were confirmed to act as RFBs *invivo* (See Figures 4 and 5). (**B**) Map of the 3705-bp linear fragment generated by digestion of pYAC_AC_10rRFBs+ with SwaI and BamHI showing the relative position of the ten putative RFBs. (**C**) Map of the 5194-bp linear fragment generated by digestion of pYAC_AC_10rRFBs+ with EcoRV and MluI showing the relative position of the 10 putative RFBs. (**D**) 2D gel immunogram of the RIs corresponding to the SwaI-BamHI 3705 bp linear fragment with its diagrammatic interpretation in (**E**). The 2D gel immunogram of the RIs corresponding to the EcoRV-MluI 5194 bp linear fragment is shown in (**F**) with its diagrammatic interpretation in (**G**). The densitometric profile corresponding to the six most distal spots observed on the simple-Y arc shown in (**D**) is presented in (**H**) indicating the height of the peaks. For comparison, the densitometric profile corresponding to the 3705-bp SwaI-BamHI of pYAC_AC_10rRFBs isolated from the top2-td strain shown in Figure 4H is presented on top.

FOB1 overexpression was responsible for the differences observed.

DISCUSSION

The rDNA of *S. cerevisiae* contains two closely spaced polar RFBs

Although the rDNA of *S. cerevisiae* is probably the best characterized so far (20), there is still controversy as to whether replication forks stall at two or three potential barriers in this *locus*. High-resolution 2D gels allowed identification of two closely spaced polar barriers that stall replication forks moving toward the *35S* transcription unit in the native chromosomal *locus* as well as in extra-chromosomal circular minichromosomes (28). This observation was confirmed by systematic mutagenesis of consecutive 10-bp segments in this region and 2D gel electrophoresis (17). However, chromatin immunoprecipitation, gel shift, footprinting and atomic force microscopy assays indicated that Fob1 directly binds to three specific sequences (RFB1, RFB2 and RFB3) in this *locus*, although only two accumulation spots are detected in 2D gels probably because RFB2 and RFB3 are too close to each other (27). To solve this apparent controversy, we constructed pYAC_AC_3′rRFBs+ where the three putative Fob1 binding sites were equally separated by 40 bp (see Figure 5). High-resolution 2D gels and densitometry of the accumulated spots observed in this minichromosome compared to those observed in pYAC_MEM_3rRFBs where only 17 bp separate RFB2 and RFB3, unambiguously showed that RFB2 does not act as a barrier *in vivo*. In other words, in the rDNA of *S. cerevisiae* there are only two sites (those Kobayashi called RFB1 and RFB3) that stall replication forks in a polar manner.

Blockage of replication forks at rRFBs when occurred were permanent, but only occurred at some of the sites that are putatively able to bind Fob1

One of the most important observations made in this study was the detection of a complete simple-Y arc regardless of the number of rRFBs present (see Figures 4–6 and 7). This observation indicated that in the minichromosomes analyzed many replication forks were able to go beyond the putative rRFBs apparently undisturbed. However, the same immunograms showed that fork blockage at all the expected rRFBs was accompanied by double-Y signals indicating that replication of the fragment was completed by means of another fork moving in the opposite direction (see Figures 4–6 and 7). Altogether, these observations strongly suggested that blockage of replication forks at the budding yeast's rRFBs when occurred were permanent, but did not occur in all cases. Replication fork stalling can occur due to intrinsic or natural impediments or due to exogenous factors such as DNA damage or nucleotide pools depletion (42). In the case of natural impediments due to the binding of specific proteins such as Fob1, other proteins are known to act upon stalled forks. In *S. cerevisiae*, the products of *TOF1* and *CSM3* are known to protect and stabilize stalled forks (43). On the contrary, forks stalled due to exogenous factors often collapse leading to DNA repair and recombination processes that could compromise genomic stability (44). The putative stability of stalled forks, regardless what causes it, is still a controversial matter (45–47). The results we obtained supported the notion that forks stalled at rRFBs do not collapse right away and remain in a stable conformation at least until another fork moving in the opposite direction completes replication of the fragment.

In circular minichromosomes some replication forks are able to go beyond 10 consecutive potential rRFBs suggesting that shortage of Fob1p limits their efficiency to block replication forks

Here, we showed that in the minichromosomes analyzed a number of replication forks were able to go beyond the potential rRFBs undisturbed (see Figures 4–6 and 7). Why? In *S. cerevisiae*, Fob1p is not essential but replication forks do not stall at rRFBs in *FOB1*-deleted cells (4,18). These observations indicate that replication forks stall at rRFBs only when Fob1 is bound to its cognate site. In other words, when a replication fork confronts a potential rRFB DNA sequence that has no Fob1 bound, it goes by with no apparent difficulty. If this also happens at the chromosomal rDNA *locus*, collision of transcription and replication would take place, as it was suggested for *S. pombe* (5). Here, it was clearly shown that *swi1* and *swi3* (homologs to *TOF1* and *CSM3* in *S. cerevisiae*, respectively) are required for fork arrest at programmed rRFBs but not at the pausing site likely caused by collision of transcription and replication (5). Fork stalling at rRFBs is known to prompt recombination. However, these recombination events are tightly regulated (18,48,49), are non-mutagenic and contribute to the concerted contraction and expansion of rDNA repeats (50,51). One of the regulatory elements is the nicotinamide adenine dinucleotide (NAD)-dependent histone deacetylase Sir2 that interacts with Fob1 and Net1 to silence transcription and inhibit recombination (18,48,49,52,53). Indeed, replication fork arrest and inhibition of recombination appear to be two independent and separable functions (53,54). Mechanistically, Fob1 was proposed to promote 'chromosome kissing' to initiate rDNA homologous recombination (55). It is important to notice that *FOB1* deletion is not lethal (18,56) although polar blockage of replication forks at rDNA genes is a conserved feature despite the proteins involved are not. In any case, the observation that blockage of replication forks at rRFBs is rather inefficient might explain both, their evolutionary conservation and the need for other mechanisms to regulate the concomitant recombination events. Altogether, these observations suggest that shortage of Fob1 in the cells might limit the efficiency of potential rRFBs to block replication forks.

Overexpression of *FOB1* and neighbor DNA sequences modulate the efficiency of rRFBs to stall replication forks

In 2D gels, the intensity of the signals generated by RIs indicates their relative abundance. The simple-Y signal is twice as much intense as the bubble signal simply because the first one is generated by the advance of a single replication fork while bubbles are generated by two advancing forks. In consequence, the frequency of each specific RI in the population is larger for the former. Similarly, if a replication fork

stalls at a specific site, the relative abundance of molecules of that particular mass and shape increases. These stalled RIs will be detected as an increased darkening (spot) at a specific site along the pattern (30). In rDNA tandem repeats, the relative intensity of the spots indicating fork stalling is often correlated with their efficiency to block fork progression (5,7,13,28).

To check if the relative abundance of Fob1 increases the efficiency of potential rRFBs to stall replication forks, we used pYAC_AC_10rRFBs+ to transfect cells of a yeast strain, GAL-3HA-FOB1, that overexpresses Fob1. The results obtained indicated that overexpression of *FOB1* modulated the efficiency of 10 successive rRFBs to stall replication forks, but some of them were still able to go beyond with no apparent difficulty (see Figure 7). Curiously, densitometry of the RIs with stalled forks of pYAC_AC_10rRFBs+ isolated from top2-td cells, showed that the last spot generated by the advancing fork, marked #10, was stronger than the previous one, marked #9 (see Figure 6). The situation reversed for the same minichromosomes isolated from GAL-3HA-FOB1. Here, the darker spot corresponded to the spot marked #9. Indeed, this was observed for all five pairs of barriers. In other words, for each pair, the first one encountered by the advancing fork (marked with even numbers) was darker in the case of pYAC_AC_10rRFBs+ isolated from cells that overexpressed Fob1 (see Figure 7). This was not obvious for the minichromosomes isolated from top2-td cells (Figure 6). It is important to notice that for pYAC_MEM_3rRFBs+ and pYAC_AC_3′rRFBs+ isolated from top2-td cells, the first barrier encountered by the advancing fork, marked RFB1 was darker in both cases (see Figures 4 and 5). This observation was confirmed for both digestions in both minichromosomes. The situation is comparable to the observations made for the rDNA repeats in *S. pombe* (5,7,8) and cultured mouse cells (12,13). Why does the situation change when five tandem repeats of the 186-bp subfragment 7 (see Figure 1C) described by Kobayashi (27) containing 10 active rRFBs were present? Brewer *et al*. suggested that the first barrier encountered by the advancing fork appears stronger because more forks reach it, or that additional sequences besides the Fob1 binding ones might be essential to build a fully wild-type barrier (28). This latter hypothesis would explain why the second barrier encountered by the progressing fork was weaker in pYAC_MEM_3rRFBs+ and pYAC_AC_3′rRFBs+ isolated from top2-td cells (Figures 4 and 5) but not in pYAC_AC_10rRFBs isolated from the same cells (Figure 6). The DNA sequence needed for the barriers named with uneven numbers to be fully competent was absent in the 186-bp subfragment 7 described by Kobayashi (27). However, the situation reversed back when Fob1 was overexpressed (Figure 7). This observation strongly suggested that for the budding yeast rRFBs to be fully active in addition to extra sequences besides the Fob1 binding ones, the relative abundance of Fob1 modulates the efficiency of rRFBs to stall replication forks. How could these protein-mediated interactions between DNA sites be mechanistically explained? ‘Chromosome kissing’ refers to protein-mediated relevant interactions between two sites located on either different chromosomes or the same chromosome (55,57). However, for these interactions to take place, all the potential DNA sites must have the putative protein bound. We speculate that DNA sequences surrounding the putative binding sites could affect the potential wrapping of DNA around Fob1 (27). This binding, though, would depend on the availability of the protein, that would at the end modulate ‘chromosome kissing’ to turn potential rRFBs into active replication fork stalling sites.

SUPPLEMENTARY DATA

Supplementary Data are available at NAR Online.

ACKNOWLEDGEMENTS

We acknowledge plasmids and DNA sequence data to Bonita Brewer, Luis Aragón, Jonathan Baxter and Takehiko Kobayashi. The authors also acknowledge Alicia Rodríguez-Bernabé for technical help.

FUNDING

Spanish Ministerio de Economía y Competitividad [BFU2014-56835 to J.B.S.]. Funding for open access charge: Spanish Ministerio de Economía y Competitividad [BFU2014-56835].
Conflict of interest statement. None declared.

REFERENCES

1. Brewer,B.J. and Fangman,W.L. (1988) A replication fork barrier at the 3′ end of yeast ribosomal RNA genes. *Cell*, **55**, 637–643.
2. Linskens,M.H.K. and Huberman,J.A. (1988) Organization of replication of ribosomal DNA in Saccharomyces cerevisiae. *Mol. Cell. Biol.*, **8**, 4927–4935.
3. Hernández,P., Martín-Parras,L., Martínez-Robles,M.L. and Schvartzman,J.B. (1993) Conserved features in the mode of replication of eukaryotic ribosomal RNA genes. *EMBO J.*, **12**, 1475–1485.
4. Kobayashi,T. and Horiuchi,T. (1996) A yeast gene product, Fob1 protein, required for both replication fork blocking and recombinational hotspot activities. *Genes Cells*, **1**, 465–474.
5. Krings,G. and Bastia,D. (2004) swi1- and swi3-dependent and independent replication fork arrest at the ribosomal DNA of Schizosaccharomyces pombe. *Proc. Natl. Acad. Sci. U.S.A.*, **101**, 14085–14090.
6. Krings,G. and Bastia,D. (2005) Sap1p binds to Ter1 at the ribosomal DNA of Schizosaccharomyces pombe and causes polar replication fork arrest. *J. Biol. Chem.*, **280**, 39135–39142.
7. Mejia-Ramirez,E., Sanchez-Gorostiaga,A., Krimer,D.B., Schvartzman,J.B. and Hernandez,P. (2005) The mating type switch-activating protein Sap1 Is required for replication fork arrest at the rRNA genes of fission yeast. *Mol. Cell. Biol.*, **25**, 8755–8761.
8. Sánchez-Gorostiaga,A., López-Estraño,C., Krimer,D.B., Schvartzman,J.B. and Hernández,P. (2004) Transcription termination factor reb1p causes two replication fork barriers at its cognate sites in fission yeast ribosomal DNA in vivo. *Mol. Cell. Biol.*, **24**, 398–406.
9. Grummt,I., Rosenbauer,H., Niedermeyer,I., Maier,U. and Ohrlein,A. (1986) A repeated 18 bp sequence motif in the mouse rDNA spacer mediates binding of a nuclear factor and transcription termination. *Cell*, **45**, 837–846.
10. Little,R.D., Platt,T.H.K. and Schildkraut,C.L. (1993) Initiation and termination of DNA replication in human rRNA genes. *Mol. Cell. Biol.*, **13**, 6600–6613.
11. Pfleiderer,C., Smid,A., Bartsch,I. and Grummt,I. (1990) An undecamer DNA sequence directs termination of human ribosomal gene transcription. *Nucleic Acids Res.*, **18**, 4727–4736.
12. Gerber,J.K., Gogel,E., Berger,C., Wallisch,M., Muller,F., Grummt,I. and Grummt,F. (1997) Termination of mammalian rDNA

replication: Polar arrest of replication fork movement by transcription termination factor TTF-I. *Cell*, **90**, 559–567.
13. López-Estraño,C., Schvartzman,J.B., Krimer,D.B. and Hernández,P. (1998) Co-localization of polar replication fork barriers and rRNA transcription terminators in mouse rDNA. *J. Mol. Biol.*, **277**, 249–256.
14. Rothstein,R., Michel,B. and Gangloff,S. (2000) Replication fork pausing and recombination or ''gimme a break''. *Genes Dev.*, **14**, 1–10.
15. Kobayashi,T., Heck,D.J., Nomura,M. and Horiuchi,T. (1998) Expansion and contraction of ribosomal DNA repeats in Saccharomyces cerevisiae: requirement of replication fork blocking (Fob1) protein and the role of RNA polymerase I. *Genes Dev.*, **12**, 3821–3830.
16. Ritossa,F.M. (1968) Unstable redundancy of genes for ribosomal RNA. *Proc. Natl. Acad. Sci. U.S.A.*, **60**, 509–516.
17. Ward,T.R., Hoang,M.L., Prusty,R., Lau,C.K., Keil,R.L., Fangman,W.L. and Brewer,B.J. (2000) Ribosomal DNA replication fork barrier and HOT1 recombination hot spot: shared sequences but independent activities. *Mol. Cell. Biol.*, **20**, 4948–4957.
18. Benguria,A., Hernandez,P., Krimer,D.B. and Schvartzman,J.B. (2003) Sir2p suppresses recombination of replication forks stalled at the replication fork barrier of ribosomal DNA in Saccharomyces cerevisiae. *Nucleic Acids Res.*, **31**, 893–898.
19. Deshpande,A.M. and Newlon,C.S. (1996) DNA replication fork pause sites dependent on transcription. *Science*, **272**, 1030–1033.
20. Kobayashi,T. (2014) Ribosomal RNA gene repeats, their stability and cellular senescence. *Proc. Jpn Acad. Ser. B Phys. Biol. Sci.*, **90**, 119–129.
21. Petes,T.D. (1979) Yeast ribosomal DNA genes are located on chromosome XII. *Proc. Natl. Acad. Sci. U.S.A.*, **76**, 410–414.
22. Ivessa,A.S. and Zakian,V.A. (2002) To fire or not to fire: origin activation in Saccharomyces cerevisiae ribosomal DNA. *Genes Dev.*, **16**, 2459–2464.
23. Muller,M., Lucchini,R. and Sogo,J.M. (2000) Replication of yeast rDNA initiates downstream of transcriptionally active genes. *Mol. Cell*, **5**, 767–777.
24. Elias-Arnanz,M. and Salas,M. (1999) Resolution of head-on collisions between the transcription machinery and bacteriophage Phi 29 DNA polymerase is dependent on RNA polymerase translocation. *EMBO J.*, **18**, 5675–5682.
25. Liu,B. and Alberts,B.M. (1995) Head-on collision between a DNA replication apparatus and RNA polymerase transcription complex. *Science*, **267**, 1131–1137.
26. Olavarrieta,L., Hernández,P., Krimer,D.B. and Schvartzman,J.B. (2002) DNA knotting caused by head-on collision of transcription and replication. *J. Mol. Biol.*, **322**, 1–6.
27. Kobayashi,T. (2003) The replication fork barrier site forms a unique structure with Fob1p and inhibits the replication fork. *Mol. Cell. Biol.*, **23**, 9178–9188.
28. Brewer,B.J., Lockshon,D. and Fangman,W.L. (1992) The arrest of replication forks in the rDNA of yeast occurs independently of transcription. *Cell*, **71**, 267–276.
29. Brewer,B.J. and Fangman,W.L. (1987) The localization of replication origins on ARS plasmids in S. cerevisiae. *Cell*, **51**, 463–471.
30. Friedman,K.L. and Brewer,B.J. (1995) Analysis of replication intermediates by two-dimensional agarose gel electrophoresis. *Methods Enzymol.*, **262**, 613–627.
31. Martín-Parras,L., Hernández,P., Martínez-Robles,M.L. and Schvartzman,J.B. (1991) Unidirectional replication as visualized by two-dimensional agarose gel electrophoresis. *J. Mol. Biol.*, **220**, 843–853.
32. Schvartzman,J.B., Martinez-Robles,M.L., Lopez,V., Hernandez,P. and Krimer,D.B. (2012) 2D gels and their third-dimension potential. *Methods*, **57**, 170–178.
33. Cebrian,J., Monturus,E., Martinez-Robles,M.L., Hernandez,P., Krimer,D.B. and Schvartzman,J.B. (2014) Topoisomerase 2 is dispensable for the replication and segregation of small yeast artificial chromosomes (YACs). *PLoS One*, **9**, e104995.
34. Ito,H., Fukuda,Y., Murata,K. and Kimura,A. (1983) Transformation of intact yeast cells treated with alkali cations. *J Bacteriol.*, **153**, 163–168.
35. Tanaka,S. and Diffley,J.F. (2002) Interdependent nuclear accumulation of budding yeast Cdt1 and Mcm2-7 during G1 phase. *Nat. Cell Biol.*, **4**, 198–207.
36. Baxter,J., Sen,N., Martinez,V.L., De Carandini,M.E., Schvartzman,J.B., Diffley,J.F. and Aragon,L. (2011) Positive supercoiling of mitotic DNA drives decatenation by topoisomerase II in eukaryotes. *Science*, **331**, 1328–1332.
37. Huberman,J.A., Spotila,L.D., Nawotka,K.A., El-Assouli,S.M. and Davis,L.R. (1987) The in vivo replication origin of the yeast 2 mm plasmid. *Cell*, **51**, 473–481.
38. Olavarrieta,L., Martínez-Robles,M.L., Hernández,P., Krimer,D.B. and Schvartzman,J.B. (2002) Knotting dynamics during DNA replication. *Mol. Microbiol.*, **46**, 699–707.
39. Santamaria,D., Viguera,E., Martinez-Robles,M.L., Hyrien,O., Hernandez,P., Krimer,D.B. and Schvartzman,J.B. (2000) Bi-directional replication and random termination. *Nucleic Acids Res.*, **28**, 2099–2107.
40. Viguera,E., Rodríguez,A., Hernández,P., Krimer,D.B., Trellez,O. and Schvartzman,J.B. (1998) A computer model for the analysis of DNA replication intermediates by two-dimensional agarose gel electrophoresis. *Gene*, **217**, 41–49.
41. Schvartzman,J.B., Martinez-Robles,M.L., Hernandez,P. and Krimer,D.B. (2010) Plasmid DNA replication and topology as visualized by two-dimensional agarose gel electrophoresis. *Plasmid*, **63**, 1–10.
42. Mirkin,E.V. and Mirkin,S.M. (2007) Replication fork stalling at natural impediments. *Microbiol. Mol. Biol. Rev.*, **71**, 13–35.
43. Calzada,A., Hodgson,B., Kanemaki,M., Bueno,A. and Labib,K. (2005) Molecular anatomy and regulation of a stable replisome at a paused eukaryotic DNA replication fork. *Genes Dev.*, **19**, 1905–1919.
44. Freidberg,E.C., Walker,G.C., Siede,W., Wood,R.D., Schultz,R.A. and Ellenberger,T. (2005) *DNA repair and mutagenesis*. 2nd edn. ASM, Washington, D.C.
45. Cox,M.M., Goodman,M.F., Kreuzer,K.N., Sherratt,D.J., Sandler,S.J. and Marians,K.J. (2000) The importance of repairing stalled replication forks. *Nature*, **404**, 37–41.
46. Labib,K. and Hodgson,B. (2007) Replication fork barriers: pausing for a break or stalling for time? *EMBO Rep.*, **8**, 346–353.
47. Mettrick,K.A. and Grainge,I. (2016) Stability of blocked replication forks in vivo. *Nucleic Acids Res.*, **44**, 657–668.
48. Gasser,S.M. and Cockell,M.M. (2001) The molecular biology of the SIR proteins. *Gene*, **279**, 1–16.
49. Gottlieb,S. and Esposito,R.E. (1989) A new role for a yeast transcriptional silencer gene, SIR2, in regulation of recombination in ribosomal DNA. *Cell*, **56**, 771–776.
50. Ide,S., Miyazaki,T., Maki,H. and Kobayashi,T. (2010) Abundance of ribosomal RNA gene copies maintains genome integrity. *Science*, **327**, 693–696.
51. Tsang,E. and Carr,A.M. (2008) Replication fork arrest, recombination and the maintenance of ribosomal DNA stability. *DNA Repair*, **7**, 1613–1623.
52. Straight,A.F., Shou,W.Y., Dowd,G.J., Turck,C.W., Deshaies,R.J., Johnson,A.D. and Moazed,D. (1999) Net1, a Sir2-associated nucleolar protein required for rDNA silencing and nucleolar integrity. *Cell*, **97**, 245–256.
53. Zaman,S., Choudhury,M., Jiang,J.C., Srivastava,P., Mohanty,B.K., Danielson,C., Humphrey,S.J., Jazwinski,S.M. and Bastia,D. (2016) Mechanism of regulation of intrachromatid recombination and long-range chromosome interactions in Saccharomyces cerevisiae. *Mol. Cell. Biol.*, **36**, 1451–1463.
54. Bairwa,N.K., Zzaman,S., Mohanty,B.K. and Bastia,D. (2010) Replication fork arrest and rDNA silencing are two independent and separable functions of the replication terminator protein Fob1 of Saccharomyces cerevisiae. *J. Biol. Chem.*, **285**, 12612–12619.
55. Choudhury,M., Zaman,S., Jiang,J.C., Jazwinski,S.M. and Bastia,D. (2015) Mechanism of regulation of 'chromosome kissing' induced by Fob1 and its physiological significance. *Genes Dev.*, **29**, 1188–1201.
56. Defossez,P.A., Prusty,R., Kaeberlein,M., Lin,S.J., Ferrigno,P., Silver,P.A., Keil,R.L. and Guarente,L. (1999) Elimination of replication block protein Fob1 extends the life span of yeast mother cells. *Mol. Cell*, **3**, 447–455.
57. Singh,S.K., Sabatinos,S., Forsburg,S. and Bastia,D. (2010) Regulation of replication termination by Reb1 protein-mediated action at a distance. *Cell*, **142**, 868–878.